Nanotechnology **21** (2010) 235201 (6pp) doi:10.1088/0957-4484/21/23/235201

Resonant and nonresonant plasmonic nanoparticle enhancement for thin-film silicon solar cells

Yu A Akimov and W S Koh

Advanced Photonics and Plasmonics Team, Computational Electronics and Photonics Programme, Institute of High Performance Computing, 1 Fusionopolis Way, # 16-16 Connexis, 138632, Singapore

E-mail: kohws@ihpc.a-star.edu.sg

Received 19 April 2010
Published 13 May 2010
Online at stacks.iop.org/Nano/21/235201

Abstract

This paper investigates the influence of resonant and nonresonant plasmonic nanostructures, such as arrays of silver and aluminum nanoparticles in the forward scattering configuration, on the optical absorption in a thin-film amorphous silicon solar cell. It is demonstrated that nonresonant coupling of the incident sunlight with aluminum nanoparticles results in higher optical absorption in the photoactive region than resonant coupling with silver nanoparticle arrays. In addition, aluminum nanoparticles are shown to maintain a net positive enhancement of the optical absorption in amorphous silicon, as compared to a negative effect by silver nanoparticles, when the nanoparticles are oxidized.

(Some figures in this article are in colour only in the electronic version)

1. Introduction

Recent research into the field of plasmonic photovoltaics has found an attractive approach that uses scattering from metallic nanostructures deposited on top of thin-film solar cells to improve light trapping and energy conversion efficiency of the cells. Through excitation of the surface plasmons, the collective oscillations of the conduction electrons in metals, the incident light may interact with the nanostructures in a resonant manner, scattering the light over a cross-sectional area larger than its geometric cross section [1]. Thus, for plasmonic nanostructures located close to the cell surface, a significant part of the scattered sunlight can be coupled with the trapped waveguide modes of the photoactive layer [2–4], improving the cell's optical absorption and giving rise to a stronger photocurrent response.

The crucial role in the observed enhancements is due to the proper selection of the nanoparticle parameters [4–6], such as shape, size and surface density, which in turn determine the scattering efficiency of the nanostructure. By changing these parameters one can tune the frequency response of the metal nanostructure and optimize the performance of the cell up to a certain limit [7]. Generally, this limit is determined by optical properties of the nanoparticle material and varies in a broad range, depending on the metal. Thus, the most important factor defining the efficiency of coupling for the scattered sunlight and the semiconductor is the proper selection of the metal used for nanostructure deposition/fabrication. Depending on the density of conduction electrons, metals can feature very different optical responses and exhibit a quite broad range of surface plasmon frequencies—from the near-infrared to the ultraviolet band [1]. As a result, the commonly used plasmonic metals may interact with the sunlight in very different ways.

In general, to maximize the efficiency of coupling with the photoactive layer, the metallic nanostructures are designed to exhibit small parasitic absorption and high scattering in the optical frequency range. Currently, silver (Ag) is considered as the most effective material among the resonant plasmonic metals, whose surface plasmons lie in the visible range. It is frequently used in various plasmonic applications, from enhanced fluorescence and Raman scattering [8, 9] to integrated optics and biosensing [10, 11]. For thin-film solar cells enhanced with resonant metallic nanostructures, Ag is also the material of choice [12–15]. It exhibits lower parasitic absorption and better coupling with the photoactive region than the other commonly used resonant plasmonic metals, such as gold and copper [2]. Nonetheless, it is still not clear whether resonant materials are indeed superior to nonresonant

plasmonic metals, such as aluminum (Al), whose surface plasmon resonances lie outside the solar spectrum, to improve the optical absorption in the photoactive region.

In fact, resonant coupling of the incident sunlight with the nanoparticle surface plasmons also leads to a drastic parasitic absorption inside the nanoparticles [7, 16]. This absorption, being unwanted losses, decreases the energy conversion efficiency and significantly limits the improvement of the photoactive region's optical absorption by the resonant nanostructures [15, 16]. On the other hand, nonresonant plasmonic metals do not exhibit high plasmon-induced losses, as their surface plasmons cannot couple with the sunlight. In other words, nonresonant metals feature much lower parasitic absorption in the optical frequency range, as compared to resonant ones. Moreover, nonresonant metals are characterized with a higher density of conduction electrons, resulting in highly negative dielectric permittivity. It makes them more suitable for the forward scattering configuration [16]. Based on this, one can expect that nonresonant Al nanostructures may provide comparable or even better enhancement of the photocurrent than Ag nanostructures. Furthermore, Al is preferred in the actual fabrication of thin-film solar cells as it is a CMOS-compatible material, as opposed to Ag, which is not CMOS-compatible.

Apart from comparing the performance of Ag and Al plasmonic nanoparticles, the stability of their enhancement is also an important consideration. Note that the studies performed so far have ignored oxidation of the plasmonic nanostructures used to enhance thin-film solar cells. However, it should be taken into account, since the nanoparticle oxidation might degrade the performance of the cell even if it is encapsulated. Thus, the impact of the oxide shell covering the metallic nanoparticles must be studied to determine the actual nanoparticle enhancement after the prolonged action of the air and moisture.

In this paper, we study the resonant and nonresonant coupling of the incident sunlight with Ag (resonant) and Al (nonresonant) plasmonic nanoparticles on the optical absorption of the photoactive layer for a thin-film hydrogenated amorphous silicon (a-Si:H) solar cell. The comparison of the resonant and nonresonant mechanisms will clarify the role of the surface plasmons in the enhanced light trapping and optical absorption of the cells. Optimization of the nanoparticle geometric parameters will allow us to improve the effect of plasmonic nanoparticles on the performance of nanoparticle-enhanced thin-film solar cells and provide a fair comparison of the optimal configurations for both Ag and Al nanoparticle arrays. Additionally, we will gauge and analyze the cause of the reduction in the optical absorption of the nanoparticle-enhanced thin-film solar cells when the nanoparticles made of Ag or Al oxidize in the presence of air and moisture.

2. Simulation model

In our simulation model, we consider a simple thin-film a-Si:H solar cell with a 240 nm thick a-Si:H layer sandwiched between a 20 nm thick transparent top conductor, ITO, and an aluminum bottom electrode of 80 nm thickness. Spherical nanoparticles of radius R are placed on top of ITO in a square lattice arrangement. The surface coverage parameter η is introduced to describe the percentage of the overall surface area of ITO covered by the nanoparticles. The model structure is illuminated by monochromatic plane waves perpendicular to the top surface, with the frequency ω and spectral power flux $F(\omega)$ corresponding to the AM1.5G solar spectrum. The full set of 3D Maxwell's equations:

$$\nabla \times \vec{E} = \mathrm{i}\omega\mu_0\vec{H}, \qquad \nabla \times \vec{H} = -\mathrm{i}\omega\varepsilon_0\varepsilon\vec{E} \tag{1}$$

are solved in COMSOL Multiphysics [17] with the dielectric permittivities $\varepsilon(\omega)$ taken from the SOPRA database [18]. The optical data for silver oxide (Ag_2O) used in the oxidation study are taken from [19].

To measure the effectiveness of optical absorption by the photoactive region and the nanoparticles, we calculate the spectral absorption rates

$$A(\omega) = \frac{Q_{\mathrm{abs}}(\omega)}{Q_{\mathrm{inc}}(\omega)}, \tag{2}$$

where $Q_{\mathrm{inc}} = SF(\omega)$ is the spectral power coming from the Sun over the solar cell surface S; $Q_{\mathrm{abs}}(\omega)$ is the spectral power absorbed by each element (the active layer or nanoparticles), defined as the integral over the element volume V:

$$Q_{\mathrm{abs}}(\omega) = \frac{\omega\varepsilon_0}{2}\int_V \mathrm{Im}[\varepsilon(\omega)]|E|^2\,\mathrm{d}V. \tag{3}$$

The calculated spectral absorption rates $A(\omega)$ characterize the part of the incident spectral power Q_{inc} absorbed in different regions. Then the total power absorbed by different components can be computed as

$$Q_{\mathrm{abs}}^{\mathrm{tot}} = \int A(\omega)F(\omega)\,\mathrm{d}\omega. \tag{4}$$

Note that total power $Q_{\mathrm{abs}}^{\mathrm{tot}}$ absorbed by the photoactive region is sensitive to the nanoparticle's geometric parameters. In order to determine the array parameters which maximize it for the a-Si:H layer, the nanoparticle radius R and coverage η are optimized, as described in [7]. To measure the improvement caused by nanoparticles, we calculate the enhancement of the total power absorbed in the active region relative to the reference case of the thin-film a-Si:H solar cell without any nanoparticle array, i.e. $Q_{\mathrm{abs}}^{\mathrm{tot}}(\text{with nanoparticles})/Q_{\mathrm{abs}}^{\mathrm{tot}}(\text{without nanoparticles}) - 1$.

3. Results and discussion

3.1. Spectral absorption

The spectral absorption rates of the a-Si:H active region and the nanoparticle array in the reference cell and cells enhanced with Ag and Al nanoparticles are shown in figure 1 for two different array configurations of small and large nanoparticles. For these configurations, the nanoparticle array parameters (R and η) were chosen such that the resonant effect of Ag nanoparticles on the optical absorption in the a-Si:H active region is maximized [7]. The small nanoparticle configuration

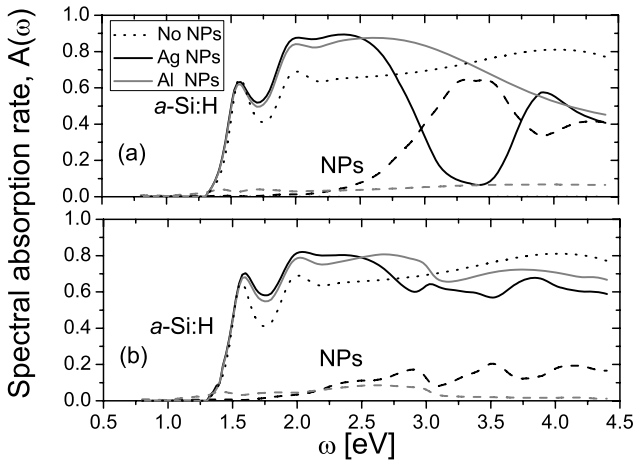

Figure 1. Spectral absorption rate $A(\omega)$ of the a-Si:H photoactive region (solid lines) and the nanoparticle array (dashed lines) in a cell enhanced with Ag and Al nanoparticles of (a) radius $R = 30$ nm and coverage $\eta = 33\%$, and (b) $R = 80$ nm and $\eta = 11\%$, as a function of frequency ω. Note that the corresponding R and η are the nanoparticle array parameters maximizing the enhancement by Ag nanoparticles through excitation of the dipolar mode (the small nanoparticles) and the multi-polar modes (the large nanoparticles). The spectral absorption rate $A(\omega)$ as a function of ω of the reference case (without nanoparticle array) is shown in the figures as dotted lines.

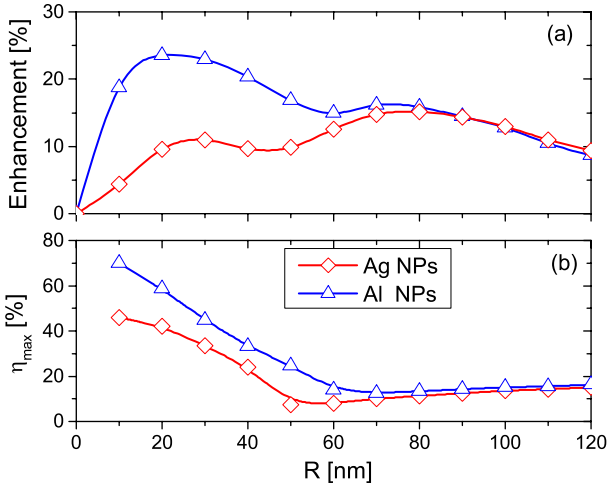

Figure 2. (a) Maximum enhancement of the optical absorption in the a-Si:H region (as compared to the reference cell), as a function of nanoparticle radius R and (b) corresponding optimum coverage η_{max} to attain the maximum enhancement, as a function of radius R.

is characterized by $R = 30$ nm and $\eta = 33\%$, while the large nanoparticle array corresponds to the case of $R = 80$ nm and $\eta = 11\%$.

Figure 1(a) clearly shows that the spectral absorption rate of the a-Si:H photoactive layer enhanced with Ag nanoparticles is dramatically decreased for $\omega > 2.75$ eV (the red solid line). This is attributed to the parasitic plasmon-induced absorption in small Ag nanoparticles (the red dashed curve), where more than 60% of the incoming energy is dissipated. As a result, the optical absorption in the a-Si:H photoactive layer is dramatically decreased (the red solid line in figure 1(a)), even when the array parameters of Ag nanoparticles are optimized. On the other hand, Al nanoparticles exhibit much smaller absorption in the solar spectrum (the blue dashed line in figure 1(a)), since their surface plasmons lie in the ultraviolet region, where the intensity of the solar irradiance is negligibly small. Thus, even for non-optimized array parameters, the spectral absorption rate of the a-Si:H cell with Al nanoparticles is comparable or higher than that of Ag nanoparticles for the frequency range plotted in figure 1(a). The better spectral absorption rates demonstrate that nonresonant coupling of the sunlight with Al nanoparticle arrays can be more effective than resonant coupling with Ag nanoparticles.

For large nanoparticles, the effect of nonresonant coupling is not so strong compared to the case of small nanoparticles. Figure 1(b) shows the comparison of the resonant and nonresonant coupling effects for the Ag and Al nanoparticle arrays of $R = 80$ nm and $\eta = 11\%$. In this case, Ag nanoparticles feature much lower spectral absorption rates at the surface plasmon frequencies than small nanoparticles (the red dashed curve). Meanwhile, Al nanoparticles still exhibit low absorption through nonresonant coupling with the incident light. Thus, in contrast to the case of small nanoparticles, the overall absorption in the a-Si:H layer cannot be improved significantly through nonresonant coupling.

3.2. Optimization

To maximize the effect of the nonresonant Al nanoparticles on the overall power absorbed in the photoactive region, we performed optimization of the surface coverage η for different nanoparticle radii R. The advantage of the nonresonant enhancement by small Al nanoparticles is illustrated in figure 2(a). This figure shows the maximum enhancement that can be achieved by using Ag and Al nanoparticles with the radius R and the corresponding optimum surface coverage η_{max}, as plotted in figure 2(b). For small Al nanoparticles, the optimum array features with $R = 20$ nm and $\eta_{max} = 59\%$. The corresponding enhancement of the optical absorption in the a-Si:H active region is 23.5%, which is higher than that of the Ag nanoparticle array's 10% [7]. Note that, for the optimum array of large Al nanoparticles (the optimum parameters are $R = 70$ nm and $\eta = 12\%$), the maximum enhancement of the optical absorption in the a-Si:H region is comparable to that of the optimum Ag nanoparticle array with $R = 80$ nm and $\eta = 11\%$. This can be explained by the similar magnitude of the sunlight coupling with both resonant and nonresonant nanoparticles. The similar magnitude of this coupling is also manifested through a similar value of the optimum surface coverage for both Ag and Al nanoparticle arrays, as shown in figure 2(b).

3.3. Oxidation effects

Figure 2 demonstrates the improvement in optical absorption of the a-Si:H active region that we can expect if we design the array parameters for pure Ag and Al nanoparticles. However, in reality, Ag and Al oxidize readily when they come in contact with air or moisture. Therefore, there is a high chance that an oxide shell will form on the surface of the metallic nanoparticles and change the enhancement. In order to examine this change, we calculated the enhancement of the

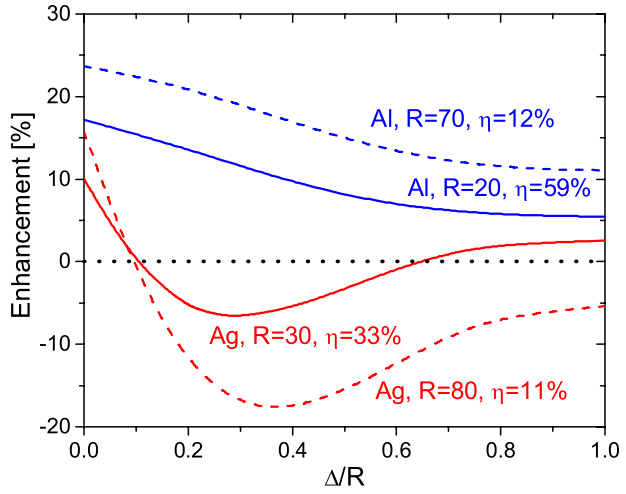

Figure 3. Enhancement of the optical absorption in the a-Si:H photoactive region, as a function of the ratio of the thickness of the oxide shell on the nanoparticle surface to the total radius of the nanoparticles. The presented nanoparticle parameters correspond to the optimized arrays of the pure Ag and Al nanoparticles.

optical absorption in the a-Si:H active region (as compared to the reference cell without any nanoparticles), as a function of the ratio of the oxide shell thickness Δ to the total radius of the nanoparticles R (figure 3), assuming that R and η of such nanoparticles do not change during oxidation.

Figure 3 shows that the degradation rates for Al nanoparticles are much smaller than those of Ag nanoparticles. For Al nanoparticles, the enhancement decreases steadily as Δ/R increases, and then saturates at the 5.5% and 11% levels for small and large Al nanoparticle arrays, respectively. Physically, this drop in enhancement is caused by a size reduction of the Al core, as Δ increases. The contribution of the oxide shell is relatively small, as Al_2O_3 is known to be transparent in the optical range. Moreover, even after complete oxidation of the Al nanoparticles, Al_2O_3 nanoparticles do give at least a 5.5% enhancement, illustrating that the Al_2O_3 nanoparticles are still good scatterers for the optimal configuration of pure Al nanoparticles.

In contrast to Al, the oxidation of Ag dramatically changes the nanoparticle enhancement: it becomes negative, when $0.1 > \Delta/R > 0.6$ and $\Delta/R > 0.1$ for small and large nanoparticles, respectively. This shows that, even with a relatively thin Ag_2O shell, the positive effect of the nanoparticles quickly becomes negative as Δ increases. Such behavior is attributed to the absorption in the Ag_2O shell, which is much more dissipative at the optical frequencies than Al_2O_3. Therefore, a combination of the reduction in the size of the Ag core and the increase in the absorption of light by the Ag_2O shell can cause the enhancement of the optical absorption of the solar spectrum to be as low as -6.7% for small Ag–Ag_2O nanoparticles and -18% for large nanoparticles. Thus, Al is a more stable nanoparticle material to enhance optical absorption in the amorphous silicon thin-film solar cell than Ag.

Although we have considered the effects of the oxide shell and the reduction of the metal core over a wide range of Δ/R, in reality the native oxide shell encapsulating the Al or Ag core is usually only several nanometers thick [19, 20]. In this range of oxide thickness, the nanoparticle enhancement degrades rapidly (especially for silver nanostructures), as observed in figure 3. Thus, it is of great interest to understand the behavior of the a-Si:H and nanoparticle spectral absorption due to the thin native oxide shell encapsulating the Ag and Al nanoparticle cores.

Figure 4 illustrates the spectral absorption rates of the a-Si:H active region and Ag nanoparticles, as functions of frequency ω, for the two optimal configurations of small and large nanoparticles with varying thickness of the silver oxide Ag_2O. One can see that the dip in the a-Si:H spectral absorption rate broadens, as the thickness of the Ag_2O shell increases (as shown in figures 4(a) and (c)). This is due to the broadening of the resonant nanoparticle absorption represented in figures 4(b) and (d). The main factors causing the broadening are: (i) the reduced size of the Ag core and (ii) the increasing thickness of the Ag_2O shell. The reduced size of the Ag core slightly shifts the surface plasmon resonance to higher frequencies ω (i.e. the right-hand side of

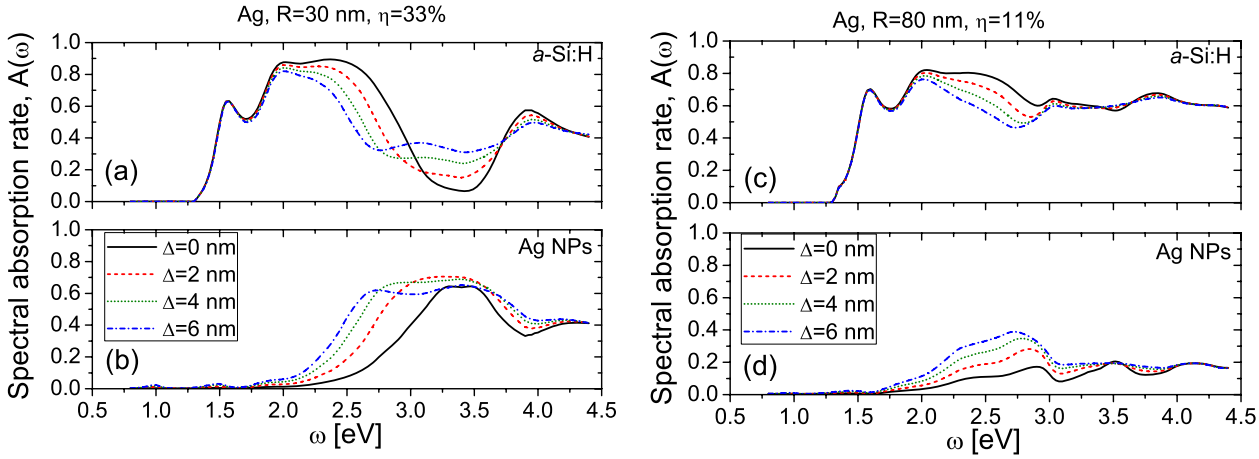

Figure 4. Spectral absorption rates $A(\omega)$ of the a-Si:H photoactive region and the Ag nanoparticle array in the cells enhanced with the nanoparticles of (a) and (b) $R = 30$ nm, $\eta = 33\%$ and (c) and (d) $R = 80$ nm, $\eta = 11\%$, as functions of frequency ω for different oxide thicknesses Δ.

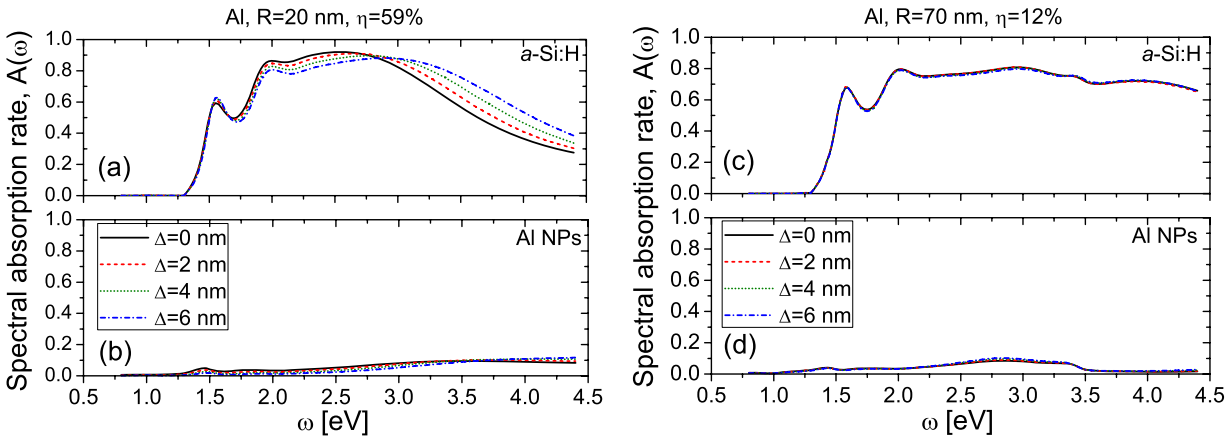

Figure 5. Spectral absorption rates $A(\omega)$ of the a-Si:H photoactive region and the Al nanoparticle array in the cells enhanced with the nanoparticles of (a) and (b) $R = 20$ nm, $\eta = 59\%$ and (c) and (d) $R = 70$ nm, $\eta = 12\%$, as functions of frequency ω for different oxide thicknesses Δ.

the absorption peak is slightly shifted to the right), while the increasing thickness of the oxide shell significantly decreases the plasmon frequencies (i.e. results in significant shift of the absorption peak to the left). A combination of these two factors results in a broader nanoparticle absorption peak. This is especially evident for small Ag nanoparticles (depicted in figure 4(b)), where the resonant nanoparticle absorption is caused mainly by the dipolar surface plasmon mode, which is most sensitive to the core and shell sizes.

The enhanced absorption inside small Ag nanoparticles significantly reduces the spectral absorption rate for the active layer, especially below 2.5 eV, where most of the solar energy is concentrated. At the same time, the real part of the dielectric permittivity of Ag_2O sharply drops below unity around 3.5 eV, leading to improved matching between the air and metal, and to reduced backward reflection from the nanoparticles. As a result, the dip formed in the a-Si:H absorption spectra by the huge resonant nanoparticle absorption becomes shallower as the thickness of the Ag_2O shell increases (figure 4(a)).

Figures 4(c) and (d) illustrate another effect of the Ag_2O shell for large Ag nanoparticles. The chosen array parameters were optimized for the pure Ag nanoparticles to minimize the nanoparticle absorption in the peak region of the solar spectrum [7]. As a result, they feature a very low spectral absorption rate (below 20%). However, the oxide formed on silver nanoparticles is highly absorbing—eventually it doubles the absorption of pure Ag nanoparticles and decreases the power absorbed in the a-Si:H layer.

In contrast to the resonant Ag nanoparticles, the spectral absorption rate of oxidized Al nanoparticles does not exhibit a huge variation, as shown in figure 5. This is primarily due to the optical characteristics of both Al and Al_2O_3: (i) the surface plasmon resonances of Al lie outside the solar spectrum; (ii) Al_2O_3 does not contribute to the nanoparticle absorption, as it is completely transparent in the optical frequency range (depicted in figures 5(b) and (d)) and (iii) the refractive index of Al_2O_3 is very low and thus the spectral distribution of the absorbed power is not changed significantly.

4. Conclusion

In conclusion, we have investigated and compared the effects of resonant and nonresonant coupling of the incident sunlight with Ag (resonant) and Al (nonresonant) nanoparticles on the optical absorption in thin-film a-Si:H solar cells. We have shown that Al is a very good candidate among the commonly used metals, which has the potential for nonresonant coupling and can double the enhancement compared to the resonant enhancement by small Ag nanoparticles for a very wide range of surface coverages η. Moreover, enhancement by Al nanoparticles only degrades slightly after oxidation, whereas Ag nanoparticles exhibit unstable enhancement and even result in a negative effect for certain ranges of oxide thicknesses due to their highly absorbing Ag_2O shell. Thus, Ag (a commonly investigated material for resonant enhancement in photovoltaic devices) is a less desirable material for nanoparticle-enhanced thin-film solar cells than Al, which relies on nonresonant coupling between the sunlight and nanoparticles.

Acknowledgments

We would like to acknowledge Professor W J R Hoefer and Dr E P Li for their valuable comments on the manuscript.

References

[1] Bohren C F and Huffman D R 1998 *Absorption and Scattering of Light by Small Particles* (New York: Wiley)
[2] Stuart H R and Hall D G 1998 *Appl. Phys. Lett.* **73** 3815
[3] Catchpole K R and Polman A 2008 *Opt. Express* **16** 21793
[4] Catchpole K R and Polman A 2008 *Appl. Phys. Lett.* **93** 191113
[5] Schaadt D M, Feng B and Yu E T 2005 *Appl. Phys. Lett* **86** 063106
[6] Akimov Yu A, Ostrikov K and Li E P 2009 *Plasmonics* **4** 107
[7] Akimov Yu A, Koh W S and Ostrikov K 2009 *Opt. Express* **17** 10195
[8] Nie S and Emory S R 1997 *Science* **275** 1102
[9] Cade N I, Ritman-Meer T, Kwakwa K A and Richards D 2009 *Nanotechnology* **20** 285201

[10] Maier S A, Brongersma M L, Kik P G, Meltzer S, Requicha A A G and Atwater H A 2001 *Adv. Mater.* **13** 1501
[11] Chen S, Svedendahl M, Kall M, Gunnarsson L and Dmitriev A 2009 *Nanotechnology* **20** 434015
[12] Moulin E, Sukmanowski J, Schulte M, Gordijn A, Royer F X and Stiebig H 2007 *Thin Solid Films* **516** 6813
[13] Pillai S, Catchpole K R, Trupke T and Green M A 2007 *J. Appl. Phys.* **101** 093105
[14] Rockstuhl C and Lederer F 2009 *Appl. Phys. Lett.* **94** 213102
[15] Nakayama K, Tanabe K and Atwater H A 2008 *Appl. Phys. Lett.* **93** 121904
[16] Akimov Yu A, Koh W S, Sian S Y and Ren S 2010 *Appl. Phys. Lett.* **96** 073111
[17] http://www.comsol.com
[18] http://www.sopra-sa.com The complex refractive index data for amorphous silicon, indium tin oxide, silver, aluminum and aluminum oxide are taken from SIAM1.mat, ITO2.mat, AG.mat, AL.mat, AL2O3.mat respectively
[19] Yin Y, Li Z-Y, Zhong Z, Gates B, Xia Y and Venkateswaran S 2002 *J. Mater. Chem.* **12** 522
[20] Langhammer C, Schwind M, Kasemo B and Zoric I 2008 *Nano Lett.* **8** 1461